

# Architecture-Controlled Synthesis of Redox-Degradable Hyperbranched Polyglycerol Block Copolymers and the Structural Implications of their Degradation

Suhyun Son,<sup>1</sup> Haeree Park,<sup>2</sup> Eeseul Shin,<sup>3</sup> Yuji Shibasaki,<sup>4</sup> Byeong-Su Kim<sup>1,3</sup>

<sup>1</sup>Department of Energy Engineering, Ulsan National Institute of Science and Technology (UNIST), Ulsan 689-798, Korea

<sup>2</sup>Department of Chemical Engineering, Ulsan National Institute of Science and Technology (UNIST), Ulsan 689-798, Korea

<sup>3</sup>Department of Chemistry, Ulsan National Institute of Science and Technology (UNIST), Ulsan 689-798, Korea

<sup>4</sup>Department of Chemistry and Bioengineering, Faculty of Engineering, Iwate University, 4-3-5 Ueda, Morioka, Iwate 020-8551, Japan

Correspondence to: B.-S. Kim (E-mail: bskim19@unist.ac.kr)

Received 27 November 2015; accepted 14 December 2015; published online 8 January 2016

DOI: 10.1002/pola.28031

**ABSTRACT:** We have successfully synthesized a series of redox-degradable hyperbranched polyglycerols using a disulfide containing monomer, 2-((2-(oxiran-2-ylmethoxy)ethyl)disulfanyl)ethan-1-ol (SSG), to yield PSSG homopolymers and hyperbranched block copolymers, P(G-*b*-SSG) and P(SSG-*b*-G), containing nondegradable glycerol (G) monomers. Using these polymers, we have explored the structures of the hyperbranched block copolymers and their related degradation products. Furthermore, side reaction such as reduction of disulfide bond during the polymerization was investigated by employing the free thiol titration experiments. We elucidated the structures of the degradation products with respect to the architecture of the

hyperbranched block copolymer under redox conditions using <sup>1</sup>H NMR and GPC measurements. For example, the degradation products of P(G-*b*-SSG) and P(SSG-*b*-G) are clearly different, demonstrating the clear distinction between linear and hyperbranched block copolymers. We anticipate that this study will extend the structural diversity of PG based polymers and aid the understanding of the structures of degradable hyperbranched PG systems. © 2016 Wiley Periodicals, Inc. *J. Polym. Sci., Part A: Polym. Chem.* **2016**, *54*, 1752–1761

**KEYWORDS:** block copolymers; hyperbranched; synthesis; polyglycerol; redox-degradable

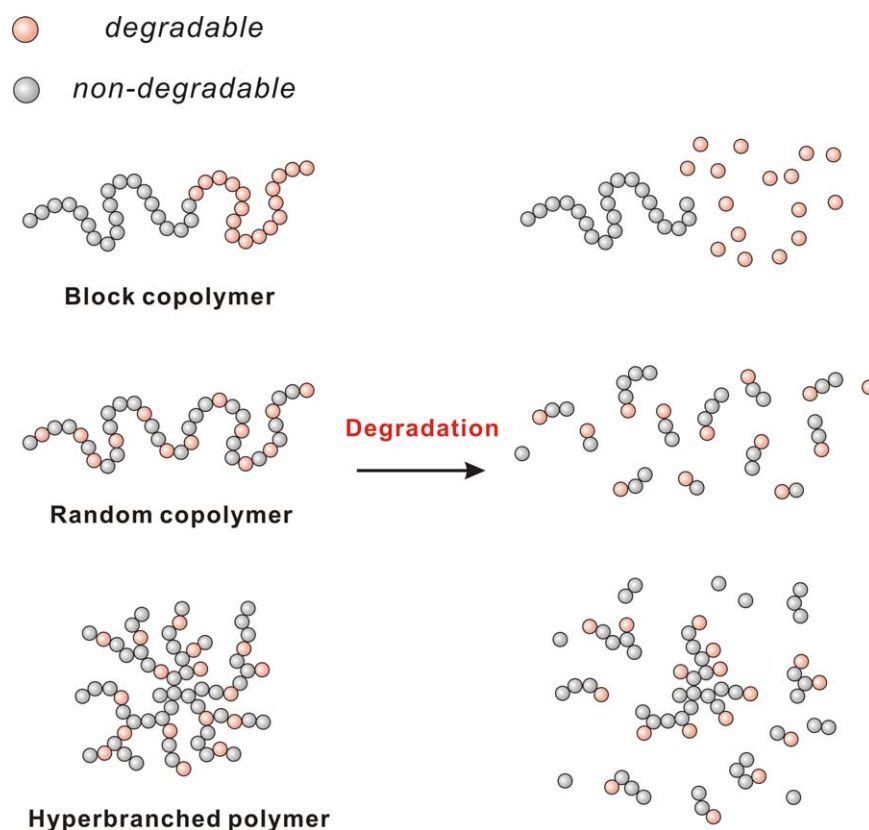
**INTRODUCTION** Hyperbranched polyglycerols (PGs) are one of the most popular hyperbranched polymers, which possess randomly branched structure with a large number of hydroxyl groups.<sup>1,2</sup> Because of their excellent biocompatibility, immunogenicity, and the large number of potential sites for further conjugation, PGs and their derivatives have attracted increasing attention for use in biomedical applications such as polymer therapeutics, human serum albumin substitutes, and proteomics.<sup>3–8</sup> Moreover, hyperbranched PGs can be prepared by a facile one-pot synthesis, even up to the kilogram scale, which assured their successful advancement to industrial levels.<sup>9,10</sup> PGs are typically synthesized by the anionic ring-opening multibranching polymerization of glycidol monomers, which can lead to a broad range of desired molecular weights from 1000 to 1,000,000 with relatively low polydispersity.

To build PGs with various architectures and versatile functionality, many functional epoxide monomers have been

developed, including ethoxyethyl glycidyl ether (EEGE), ethoxy vinyl glycidyl ether, allyl glycidyl ether (AGE), *N,N*-diisopropyl ethanolamine glycidyl ether, *N,N*-dibenzyl amino glycidol, and glycidyl propargyl ether (GPE).<sup>11–18</sup> These monomers are often copolymerized with glycidol to produce PGs with diverse structures. As a representative example, use of the EEGE monomer and a protected glycidol monomer enables to various architectures such as linear or linear-hyperbranched PGs.<sup>12,13</sup> To introduce additional functional groups, Mattson et al. have installed AGE for the subsequent functionalization with thiol-ene click chemistry.<sup>18</sup> Schüll et al. also copolymerized GPE with glycidol to obtain a multi-alkyne functional hyperbranched PG.<sup>15</sup> Furthermore, stimuli-responsive epoxide monomers can be introduced to yield degradable, hyperbranched PGs with advanced functionality. Specifically, to meet the demands of advanced biomedical applications, PG-based materials that are biocompatible yet degradable under physiological conditions are highly desirable. In that regard, acid-cleavable ketal groups or redox-

Additional Supporting Information may be found in the online version of this article.

© 2016 Wiley Periodicals, Inc.



**SCHEME 1** Degradation structure depending on the type of polymers. [Color figure can be viewed in the online issue, which is available at [wileyonlinelibrary.com](http://wileyonlinelibrary.com).]

degradable disulfide groups can be integrated into the monomer to yield a series of hyperbranched PGs that are degradable under specific biological stimuli.<sup>19–21</sup>

Installing degradable linkage groups or moieties within the polymer is an important and challenging subject; furthermore, the investigation of the degradation products can provide insight into elucidating the detailed structure of the polymers prior to degradation. Therefore, studies on a variety of degradable polymers and their degradation products have been widely conducted (Scheme 1).<sup>22–25</sup> In contrast to the considerable research on the degradation of linear polymers, there have been almost no systematic report on the synthesis and degradation of (hyper)branched polymers, possibly due to its structural complexity. Recently, some researchers studied the degradation of brush and hyperbranched polymers, for example, Engler et al. have reported polycarbonate based brush polymers bearing cleavable disulfide-linked side chains and their related degradation products.<sup>26</sup> In addition, Rikkou-Kalourkoti et al. studied the synthesis and degradation of thermolyzable hyperbranched polymers using an iminer bearing a thermolyzable acylal group.<sup>27</sup> Our group has recently developed the redox-degradable hyperbranched polyglycerols (PSSG) and studied its degradation products from the copolymerization with non-degradable glycerol monomer.<sup>21</sup> However, the study was limited to investigation of random copolymer system in which the sequence of polymerization was not controlled.

Unlike the linear block copolymer, the location of degradable linkage within the hyperbranched polymers has a significant implication after the degradation.

Thus, in continuation of our investigation into the development of hyperbranched PGs for biomedical applications, herein, we synthesized a series of redox-degradable hyperbranched PG-based polymers using a disulfide containing monomer, 2-((2-(oxiran-2-ylmethoxy)ethyl)disulfanyl)ethanol-1-ol (SSG), to yield PSSG homopolymers and block copolymers with a non-degradable glycerol (G) monomer. Hyperbranched block copolymers of P(G-*b*-SSG) and P(SSG-*b*-G) with controlled molecular weights (6210–26,590 g/mol) and relatively low polydispersity indices ( $M_w/M_n < 1.54$ ) were prepared by anionic ring-opening multibranching polymerization. We also elucidated the structural details of the degradation products from homopolymers and block copolymers of hyperbranched redox-degradable PGs under redox conditions based on <sup>1</sup>H NMR and GPC measurements. Finally, we investigated the superior biocompatibility of PSSG, P(G-*b*-SSG) and P(SSG-*b*-G) via cell viability assays.

## EXPERIMENTAL

### Materials

All reagents and solvents were purchased from either Sigma Aldrich or Acros and used as received unless otherwise

stated. Chloroform- $d_1$  and deuterium oxide were purchased from Cambridge Isotope Laboratory.

### Characterization

$^1\text{H}$  NMR spectra were acquired using a VNMRs 600 spectrometer operating at 600 MHz using  $\text{CDCl}_3$  and  $\text{D}_2\text{O}$  as solvents. The number- and weight-averaged molecular weight and molecular weight distribution were measured by gel permeation chromatography (GPC, Agilent Technologies 1200 series) using polystyrene as a standard in DMF. Measurements were carried out at 30 °C with a flow rate of 1.00 mL/min. Differential scanning calorimetry (DSC) was performed using a DSC Q200 model from TA Instruments in the temperature range of  $-80$  to 100 °C at a heating rate of 10 K/min under nitrogen. A UV-Vis spectrophotometer (UV-2550, Shimadzu) was used to measure the absorbance of iodine for the volumetric titration of free thiols.

### Synthesis of 2-{2-[2-(Oxiran-2-Ylmethoxy)Ethyl] Disulfanyl}Ethanol (SSG, Monomer), Poly(2-((2-(oxiran-2-Ylmethoxy)Ethyl)Disulfanyl) ethan-1-Ol) (PSSG Homopolymer) and Poly(glycerol-co-2-{2-[2-(oxiran-2-ylmethoxy)ethyl]disulfanyl}ethanol) (P(G-co-SSG) Copolymer)

SSG monomer, PSSG homopolymer, and P(G-co-SSG) copolymers were prepared according to the previously reported method.<sup>21</sup>

### Synthesis of Poly(glycerol-block-2-{2-[2-(oxiran-2-ylmethoxy)ethyl] disulfanyl}ethanol) (P(G<sub>130</sub>-b-SSG<sub>80</sub>) Block Copolymer, Polymer 6)

Trimethylolpropane (TMP) (24 mg, 0.179 mmol) was placed in a two-neck round-bottom flask. Potassium methoxide in methanol (25 wt%, 20  $\mu\text{L}$ , 0.0678 mmol) was diluted with 0.70 mL of methanol and then added to the flask and stirred for 30 min at room temperature under an argon atmosphere. Excess methanol was removed using a rotary evaporator and the remaining product was dried in a vacuum oven (90 °C, 3 h) to yield the initiator as a white salt. The flask was then purged with argon and heated to 90 °C. Then, glycidol (G) monomer (1.72 g, 23.2 mmol) was added dropwise over 6 h using a syringe pump. After complete addition of the monomer, the reaction was allowed to continue for an additional 1 h to yield the PG macroinitiator. Then, to this solution, SSG monomer (3.01 g, 14.3 mmol) was added dropwise over 6 h using a syringe pump. After complete addition of the monomer, the reaction was allowed to continue for an additional 1 h. The resulting P(G-b-SSG) polymer was dissolved in 1.0 mL of methanol and the homogeneous polymer solution was precipitated into excess diethyl ether and washed twice with diethyl ether. Finally, the resulting polymer was dried under vacuum at 60 °C for 2 days. The  $M_n$  of polymer **6** was 18,400 g/mol, as calculated from the NMR data shown in Figure 2(a) using the following equation: Number of repeating units (SSG) = 56.31 (integration value)  $\times$  3 (number of protons of TMP (methyl, 3H))/4 (number of protons neighboring the disulfide moiety of SSG (4H)) = 42, number of repeating units (G) = [339.92 (integration value)  $\times$  3 (num-

ber of protons of TMP (methyl, 3H)) - {(42 (number of SSG repeating units)  $\times$  9 (number of protons of SSG except those that are adjacent to the disulfide moiety (9H))) - 6 (number of protons of TMP (ether, 6H))}] / 5 (number of protons of the G monomer (5H)) = 127;  $M_n$  = 74.08 (molecular weight of the G monomer)  $\times$  127 + 210.31 (molecular weight of the SSG monomer)  $\times$  42 + 134.17 (molecular weight of TMP) = 18,400.

### Synthesis of Poly(glycerol-block-2-{2-[2-(oxiran-2-ylmethoxy) ethyl]disulfanyl}ethanol) (P(SSG<sub>30</sub>-b-G<sub>100</sub>) Block Copolymer, Polymer 9)

P(SSG<sub>30</sub>-b-G<sub>100</sub>) block copolymer was synthesized using the same strategy to prepare the P(G-b-SSG) block copolymers; however, the monomer addition sequence was reversed. The reaction mixture comprised trimethylolpropane (TMP) (24 mg, 0.179 mmol), potassium methoxide in methanol (25 wt%, 20  $\mu\text{L}$ , 0.0678 mmol) in 0.70 mL of methanol, SSG monomer (1.13 g, 5.36 mmol), and glycidol (G) monomer (1.32 g, 17.9 mmol). The  $M_n$  of polymer **9** was 14,700 g/mol, as calculated from the NMR data shown in Figure 2(b) using the following equation: Number of repeating units (SSG) = 30.53 (integration value)  $\times$  3 (number of protons of TMP (methyl, 3H))/4 (number of protons neighboring the disulfide moiety of SSG (4H)) = 23, number of repeating units (G) = [314.24 (integration value)  $\times$  3 (number of protons of TMP (methyl, 3H)) - {(31 (number of SSG repeating units considering only PSSG core)  $\times$  9 (number of protons of SSG except those that are adjacent to the disulfide moiety (9H))) - 6 (number of protons of TMP (ether, 6H))}] / 5 (number of protons of the G monomer (5H)) = 131;  $M_n$  = 74.08 (molecular weight of the G monomer)  $\times$  131 + 210.31 (molecular weight of the SSG monomer)  $\times$  23 + 134.17 (molecular weight of TMP) = 14,700.

### Characterization of Free Thiol by Iodine Titration

For titration experiments, an aqueous solution of mercaptoethanol (10.0 mM) was used to draw a standard titration curve. Specifically, 5.0  $\mu\text{L}$  of aqueous iodine solution (0.10 mM) was added dropwise to a solution of mercaptoethanol with stirring while monitoring the UV-Vis absorbance at 287 nm and 351 nm. This titration measurement afforded a standard calibration curve for the iodine titration of free thiol in solution.

### Polymer Degradation

Degradation of PSSG by disulfide reduction was studied by GPC. Dithiothreitol (DTT, 2 equiv of disulfide) was added to solutions of the PSSG homopolymer, P(G-b-SSG), and P(SSG-b-G) block copolymers in DMF and the samples were analyzed using GPC in DMF. The molecular weight and PDI were measured and the results of before and after DTT treatment were compared.

### Cytotoxicity Assay

MTT assay was performed according to the previously reported method.<sup>21</sup>

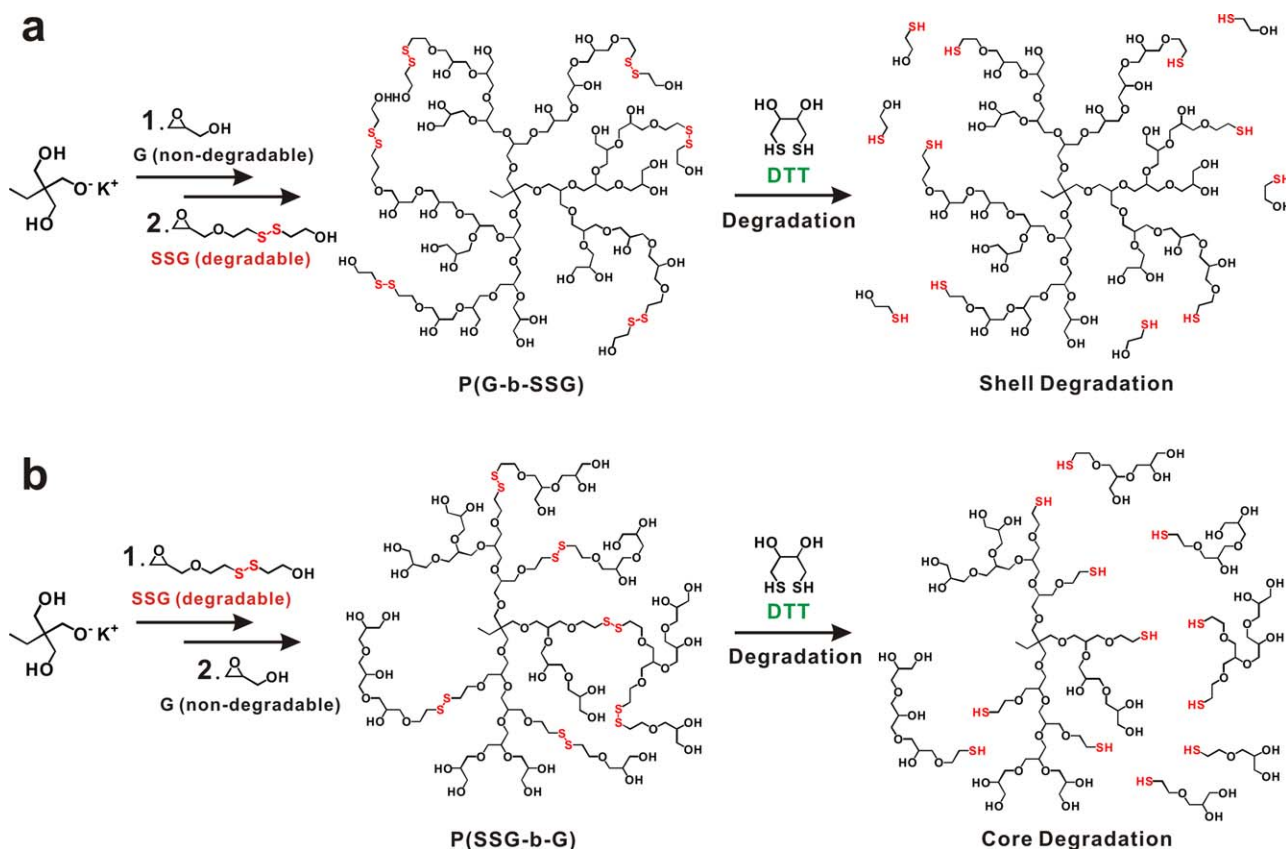


**FIGURE 1** Synthetic pathway and degradation structure of two types of redox-degradable hyperbranched block copolymers; (a) shell degradable P(G-*b*-SSG) and (b) core degradable P(SSG-*b*-G). [Color figure can be viewed in the online issue, which is available at [wileyonlinelibrary.com](http://wileyonlinelibrary.com).]

## RESULTS AND DISCUSSION

### Synthesis of Hyperbranched Block Copolymers

We synthesized two types of hyperbranched block copolymers, P(G-*b*-SSG) and P(SSG-*b*-G), by adding the different monomers in a different sequence (Fig. 1). In this report, we

employed a nondegradable glycidol (G) and SSG as a synthetic redox-degradable monomer. In clear contrast to their linear AB-type block copolymer counterpart, hyperbranched AB block copolymer can form distinctly different structures by altering the order of monomer addition during synthesis. To control the degradation products, we switched the order

**TABLE 1** Characterization Data for all Homo- and Copolymers Synthesized in this Study

No.	Polymer Composition (Target)	Polymer Composition (NMR) <sup>a</sup>	$M_n$ (Target)	%SSG (Target)	$M_n$ (NMR) <sup>a</sup>	%SSG (NMR) <sup>a</sup>	$M_n$ (GPC) <sup>b</sup>	$M_n/M_w$ (GPC) <sup>b</sup>	$T_g$ (DSC)
1	PG <sub>150</sub>	PG <sub>147</sub>	11,200	0	11,000	0	9,600	1.28	-25
2	PSSG <sub>30</sub>	PSSG <sub>31</sub>	6,440	100	6,650	100	4,230	1.39	-38
3	P(G <sub>167-co</sub> -SSG <sub>56</sub> ) P(G- <i>b</i> -SSG)	P(G <sub>114-co</sub> -SSG <sub>48</sub> )	24,190	25.1	18,700	29.6	15,800	1.28	-34
4	P(G <sub>50-b</sub> -SSG <sub>9</sub> )	P(G <sub>52-b</sub> -SSG <sub>5</sub> )	6,210	15.3	5,040	8.8	3,760	1.23	-35
5	P(G <sub>100-b</sub> -SSG <sub>10</sub> )	P(G <sub>100-b</sub> -SSG <sub>4</sub> )	9,640	9.1	8,380	3.9	7,890	1.54	-30
6	P(G <sub>130-b</sub> -SSG <sub>80</sub> ) P(SSG- <i>b</i> -G)	P(G <sub>127-b</sub> -SSG <sub>42</sub> )	26,590	38.1	18,400	24.9	12,400	1.27	-33
7	P(SSG <sub>14-b</sub> -G <sub>100</sub> )	P(SSG <sub>3-b</sub> -G <sub>97</sub> )	10,490	12.3	7,950	3.0	7,700	1.35	-32
8	P(SSG <sub>30-b</sub> -G <sub>50</sub> )	P(SSG <sub>28-b</sub> -G <sub>65</sub> )	10,150	37.5	10,800	30.1	5,680	1.39	-33
9	P(SSG <sub>30-b</sub> -G <sub>100</sub> )	P(SSG <sub>23-b</sub> -G <sub>131</sub> )	13,850	23.1	14,700	14.9	6,470	1.34	-31

<sup>a</sup> Determined via <sup>1</sup>H NMR spectroscopy.

<sup>b</sup> Obtained from GPC-RI in DMF with a polystyrene standard.

of polymerization of the two respective monomers; for example, in the case of P(G-*b*-SSG), after the hyperbranched PG macroinitiator was obtained, SSG was added to yield the P(G-*b*-SSG) copolymer. All polymers were synthesized by anionic ring-opening multibranching polymerization by using a potassium alkoxide initiator, prepared by the reaction of TMP and potassium methoxide.<sup>9</sup> As reported in our previous studies, the slow monomer addition method was used because it enabled the synthesis of hyperbranched polymers in a controlled manner.<sup>8,21</sup> Successful syntheses of homopolymers and two types of hyperbranched block copolymers were observed using <sup>1</sup>H NMR, GPC, and DSC measurement (Table 1). All synthesized PSSG-based polymers were soluble in water and polar organic solvents such as methanol, DMF, and DMSO. As shown in the <sup>1</sup>H NMR spectra, the successful polymerization was confirmed with disappearance of epoxide signal by G and SSG in each polymerization step and the characteristic peaks corresponding to the methylene groups adjacent to the disulfide moiety (peaks labeled c at 2.9–3.1 ppm) and polyether backbone signals (peaks marked d at 3.4–4.2 ppm) (Fig. 2). In Figure 2(a), we found considerable change in the disulfide signal upon additional polymerization of the SSG monomer to yield the hyperbranched block copolymer, P(G-*b*-SSG). Although new peaks were not observed for P(SSG-*b*-G), the <sup>1</sup>H NMR intensity of signals arising from the polyether backbone became stronger after addition of monomer G, indicating the growth of the polyether backbone upon polymerization of G [Fig. 2(b)]. We calculated the molecular weight and the incorporation ratio of SSG by integrating both peaks of the disulfide groups in SSG and polyether backbone against the signal of the methyl group of the TMP initiator (peak marked a at 0.8 ppm) (see the Experimental section and Supporting Information Figs. S1 and S2 for detailed calculations). Generally, we found relatively good agreement between the target and calculated molecular weights in the respective homopolymers of PG and PSSG; however, there are some discrepancies between polymer composition determined from the feed ratio and from NMR particularly for the two types of hyperbranched block copolymers (Table 1). Our previous in situ <sup>13</sup>C NMR spectroscopy measurements on bulk polymer have shown that the SSG monomer has relatively low conversion (40–55%) in comparison with plain G monomer due to its reduced reactivity. This difference in reactivity could be attributed to the structure of the disulfide spacer within SSG, which can hinder the nucleophilic attack at epoxide and, thus, reduce the reactivity of SSG during polymerization, as has been similarly observed in other studies. On the other hand, we found the lower intensity of disulfide signal after addition of G with the appearance of new peaks at 2.8 to 2.9 ppm, which could be attributed to the methylene group adjacent to the thiol and sulfonyl ester groups originated from side-reactions of the disulfide bond. For instance, after verifying the full conversion of SSG to PSSG<sub>30</sub>, it was further polymerized with G to synthesize P(SSG<sub>30</sub>-*b*-G<sub>100</sub>); however, we observed that the PSSG<sub>30</sub> (polymer 2) became P(SSG<sub>23</sub>-*b*-G<sub>131</sub>) (polymer 9) after polymerization with G monomer. This result clearly indicates the occurrence of a side reaction

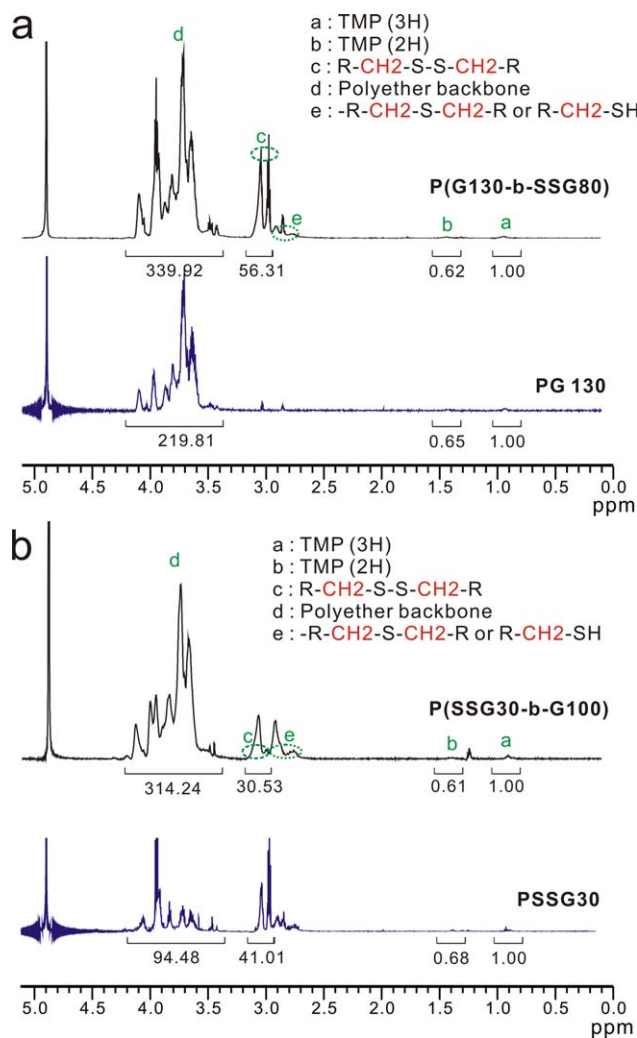


**FIGURE 2** <sup>1</sup>H NMR spectra before and after addition of the second monomer to confirm the successful synthesis of the hyperbranched block copolymers of (a) P(G<sub>130</sub>-*b*-SSG<sub>80</sub>) and (b) P(SSG<sub>30</sub>-*b*-G<sub>100</sub>). [Color figure can be viewed in the online issue, which is available at [wileyonlinelibrary.com](http://www.wileyonlinelibrary.com).]

involving the depolymerization of disulfide groups during the postpolymerization with reactive G monomer. It is postulated that the incoming alkoxide group (RO<sup>-</sup>) of the G monomer reacts with the disulfide group (R'SSR'') to yield thiolate (R'S<sup>-</sup>) and sulfonyl esters (ROSR'') during the postpolymerization with G, which will eventually degrade into thiols (R'SH and R''SH) and alcohol (ROH).<sup>28,29</sup>

In order to investigate the side reactions that occur during the polymerization of PSSG, we used free thiol titration experiments by oxidizing thiol with iodine.<sup>30,31</sup> It is known that water-soluble thiols can be readily oxidized to disulfide by aqueous iodine and results in the appearance characteristic UV-vis absorbance peaks at 287 and 351 nm.



**TABLE 2** Characterization Data for the Side Reactions of PSSG-Based Copolymers

No	Polymer Composition (Target)	Polymer Composition (NMR) <sup>a</sup>	G/SSG Ratio (Target)	G/SSG Ratio (NMR) <sup>a</sup>	No. SH in a Polymer Chain (UV-Vis) <sup>b</sup>	No. SS in a Polymer Chain (NMR) <sup>b</sup>	SH/SS%
	PSSG <sub>10</sub>	PSSG <sub>9</sub>			0.63	9	7.0
2	PSSG <sub>30</sub>	PSSG <sub>31</sub>			0.78	31	2.5
	PSSG <sub>50</sub>	PSSG <sub>53</sub>			1.30	53	2.4
	P(G- <i>b</i> -SSG)						
4	P(G <sub>50</sub> - <i>b</i> -SSG <sub>9</sub> )	P(G <sub>52</sub> - <i>b</i> -SSG <sub>5</sub> )	5.55	10.40	0.58	5	11.6
5	P(G <sub>100</sub> - <i>b</i> -SSG <sub>10</sub> )	P(G <sub>100</sub> - <i>b</i> -SSG <sub>4</sub> )	10.00	25.00	0.23	4	5.7
6	P(G <sub>130</sub> - <i>b</i> -SSG <sub>80</sub> )	P(G <sub>127</sub> - <i>b</i> -SSG <sub>42</sub> )	1.62	3.02	1.93	42	4.6
	P(SSG- <i>b</i> -G)						
7	P(SSG <sub>14</sub> - <i>b</i> -G <sub>100</sub> )	P(SSG <sub>3</sub> - <i>b</i> -G <sub>97</sub> )	7.14	32.33	3.88	3	129.3
8	P(SSG <sub>30</sub> - <i>b</i> -G <sub>50</sub> )	P(SSG <sub>28</sub> - <i>b</i> -G <sub>65</sub> )	1.66	2.32	3.94	28	14.1
9	P(SSG <sub>30</sub> - <i>b</i> -G <sub>100</sub> )	P(SSG <sub>23</sub> - <i>b</i> -G <sub>131</sub> )	3.33	5.69	10.12	23	44.0

<sup>a</sup> Determined via <sup>1</sup>H NMR spectroscopy.

<sup>b</sup> Measured using UV-Vis spectroscopy by plotting the intensity at a wavelength of 351 nm.

On the basis of the reactions presented above, we determined the amount of free thiols in PSSG homopolymers and block copolymers of P(G-*b*-SSG) and P(SSG-*b*-G) using mercaptoethanol as a reference standard (Figs. S4–S7 in the Supporting Information and Table 2). We determined that both the PSSG homopolymer and P(G-*b*-SSG) block copolymer had relatively low thiol content of around 10% free thiol to disulfide groups (i.e., SH/SS ratio) due to the side reaction during the polymerization as described earlier. In contrast, the P(SSG-*b*-G) block copolymer had a relatively high SH/SS ratio with a broad range (14 – 129%). In addition, we observed that the SH/SS ratio of P(SSG-*b*-G) depended strongly on the G/SSG ratio; that is, a high G/SSG ratio led to a greater SH/SS ratio. Also, two facts regarding this observation emerged: (i) although P(SSG<sub>30</sub>-*b*-G<sub>50</sub>) (polymer **8**) and P(SSG<sub>30</sub>-*b*-G<sub>100</sub>) (polymer **9**) were polymerized from the same PSSG<sub>30</sub> macroinitiator (polymer **2**), P(SSG<sub>30</sub>-*b*-G<sub>100</sub>) has a higher SH/SS ratio than P(SSG<sub>30</sub>-*b*-G<sub>50</sub>), and (ii) despite P(SSG<sub>14</sub>-*b*-G<sub>100</sub>) (polymer **7**) and P(SSG<sub>30</sub>-*b*-G<sub>100</sub>) (polymer **9**) having the same G composition, P(SSG<sub>14</sub>-*b*-G<sub>100</sub>) has a higher SH/SS ratio due to its high G/SSG ratio. The GPC results show that the polymerization of hyperbranched block copolymers from their respective macroinitiators, PG<sub>130</sub> and PSSG<sub>30</sub>, was successful, and the hyperbranched polymers had relatively low molecular weight distribution values ( $M_w/M_n < 1.54$ ) (Table 1). However, there are deviations between the molecular weights calculated from NMR and those obtained from GPC. This result can be explained because globular hyperbranched structure of hyperbranched PG based polymers did not contribute to the overall hydrodynamic radius of the polymers. Also, the presence of numerous hydroxyl functional groups and use of polystyrene as calibration for GPC could be the sources of the deviation between experiments.

To verify the structures of hyperbranched block copolymers and their thermal properties, we used DSC measurements

(Fig. 3). PGs are non-crystalline, flexible polymers that have glass transition temperatures ( $T_g$ ) in the range from –19 to –26 °C. In contrast, the PSSG homopolymer has a much lower  $T_g$  than those of the PGs; for example, it has a range of between –48 to –55 °C.<sup>18</sup> The lower  $T_g$  of PSSG can be accounted for by two reasons: (i) the longer-CH<sub>2</sub>CH<sub>2</sub>-S-CH<sub>2</sub>CH<sub>2</sub>-spacer unit in the PSSG monomer produces a loose structure in the polymer in comparison with the compact structure of that of PG and (ii) lower polarity and weak hydrogen bonding in PSSG can result in relatively free

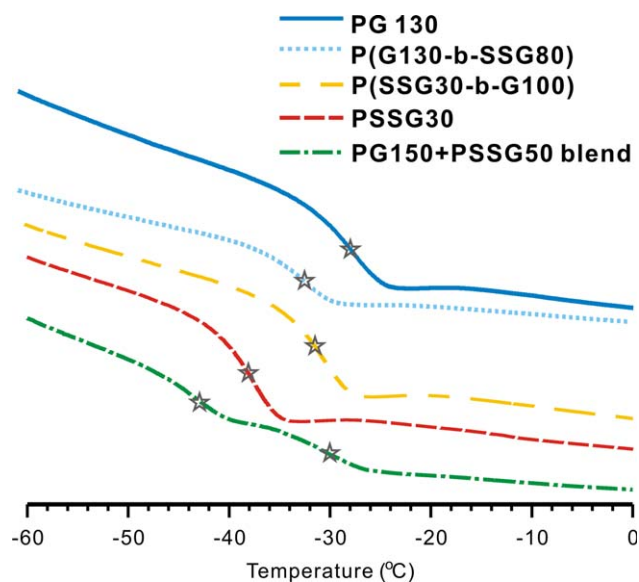


**FIGURE 3** DSC curves for PG<sub>130</sub> (blue), P(G<sub>130</sub>-*b*-SSG<sub>80</sub>) (sky blue), P(SSG<sub>30</sub>-*b*-G<sub>100</sub>) (yellow), PSSG<sub>30</sub> (red), and a simple blend of PG<sub>150</sub> and PSSG<sub>50</sub> homopolymers (green). Star marks indicate the glass transition temperatures ( $T_g$ ) for each polymer. [Color figure can be viewed in the online issue, which is available at [wileyonlinelibrary.com](http://wileyonlinelibrary.com).]

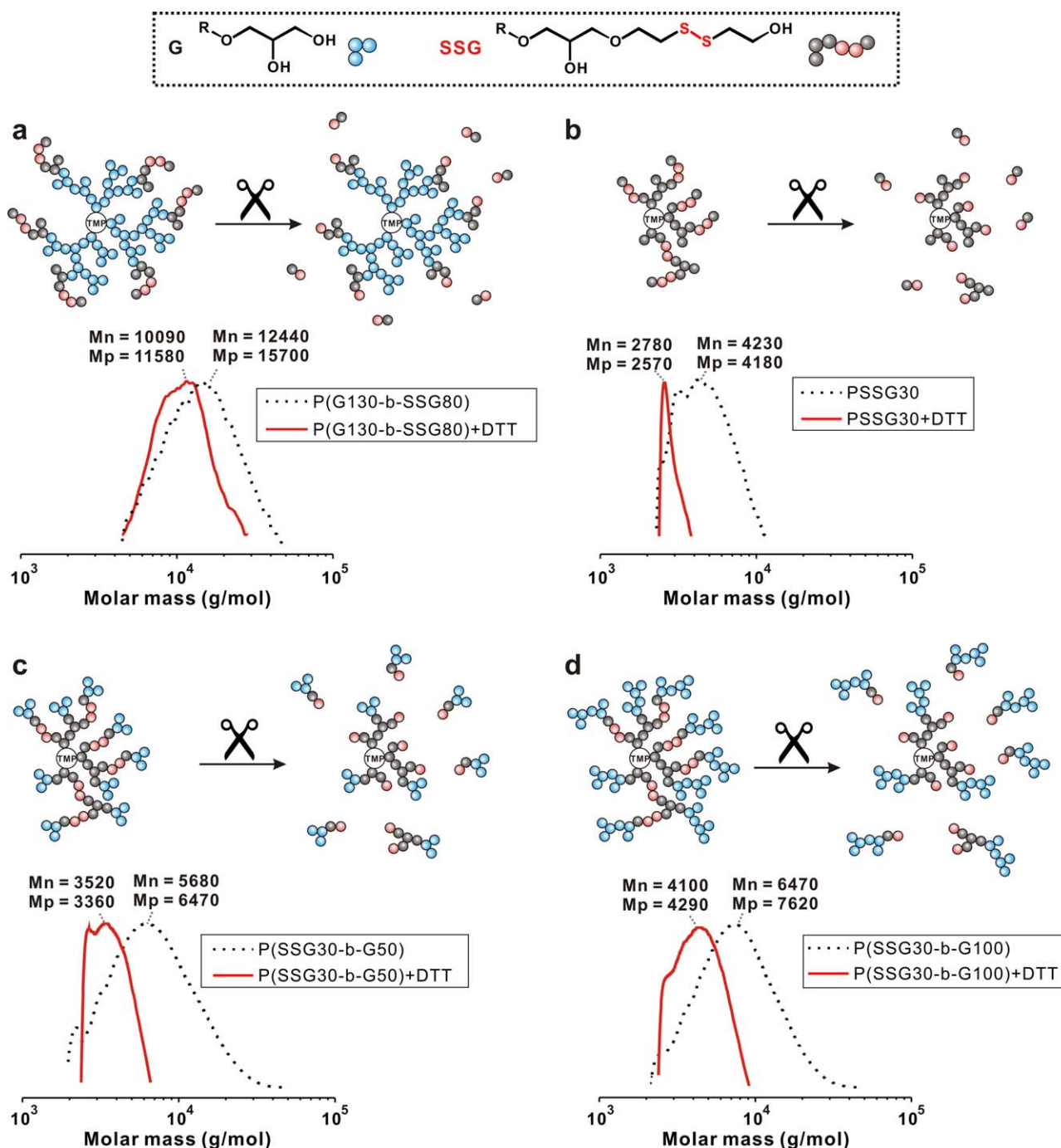


**FIGURE 4** Schematic degradation structure of PSSG polymers and the corresponding GPC traces of (a)  $P(G_{130}\text{-}b\text{-SSG}_{80})$ , (b)  $PSSG_{30}$ , (c)  $P(SSG_{30}\text{-}b\text{-G}_{50})$ , and (d)  $P(SSG_{30}\text{-}b\text{-G}_{100})$  before (black curve) and after (red curve) degradation. [Color figure can be viewed in the online issue, which is available at [wileyonlinelibrary.com](http://wileyonlinelibrary.com).]

motion of the polymer chain. Interestingly, the  $T_g$ 's of the hyperbranched block copolymers of  $P(G\text{-}b\text{-SSG})$  are located between those of PG and PSSG. For example, after polymerization to form hyperbranched  $P(G_{130}\text{-}b\text{-SSG}_{80})$ , the  $T_g$  of  $PG_{130}$  ( $-25\text{ }^\circ\text{C}$ ) shifted to  $-33\text{ }^\circ\text{C}$ . In addition, the  $T_g$  of  $PSSG_{30}$  ( $-38\text{ }^\circ\text{C}$ ) increased to  $-31\text{ }^\circ\text{C}$  in the  $P(SSG_{30}\text{-}b\text{-G}_{100})$  copolymer. It is of note that we observed only single  $T_g$  from the PSSG based hyperbranched block copolymer in

contrast to the two independent  $T_g$ 's from simple linear block copolymers. We postulate that this result is attributed to miscibility of PG and PSSG, and, more importantly, its globular hyperbranched structure even in the segregated block copolymer architecture, restricting phase separation between two blocks. As a control, we found that a simple blend of two homopolymers retained two separate  $T_g$ 's of the respective homopolymers.

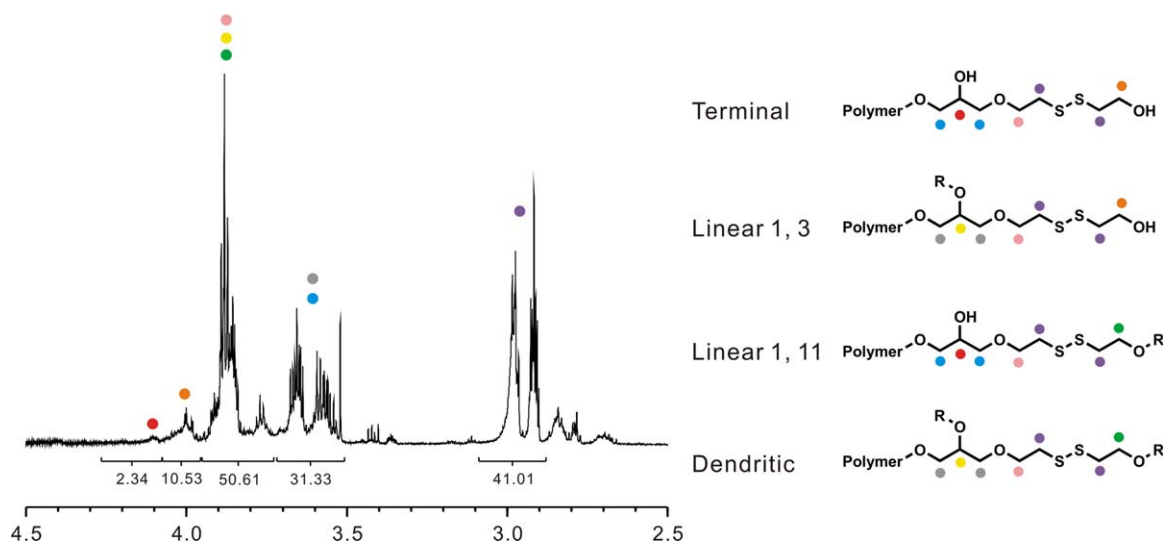


**FIGURE 5**  $^1\text{H}$  NMR spectra of PSSG<sub>30</sub> homopolymer and detailed assignments of the respective protons giving rise to these signals. [Color figure can be viewed in the online issue, which is available at [wileyonlinelibrary.com](http://wileyonlinelibrary.com).]

### Degradation Study of Two Types of Hyperbranched Block Copolymers

The presence of disulfide bonds in the polymer main chain allows their degradation by redox stimuli. It should be highlighted that SSG has a critical advantage over other degradable epoxide monomers for studies of degradable PGs. Specifically, SSG can be homopolymerized with nearly 100% conversion, while other degradable monomers generally display only low conversions (ca. 20%) during homopolymerization. By exploiting this advantage, we easily prepared both P(G-*b*-SSG) and P(SSG-*b*-G) block copolymers by changing the sequence of addition of the monomers, allowing us to explore the structures of the degradation products with respect to the architecture of the block copolymer. Firstly, we studied the degradation of the shell-degradable hyperbranched block copolymer of P(G-*b*-SSG). For this polymer, we expected that the outer shell would be degraded with a slight decrease in molecular weight. As shown in Figure 4(a), we found that the molecular weight of polymer **6** decreased slightly from 12,440 to 10,090 g/mol after degradation. Although GPC measurement with PS standards retains intrinsic limitation in determining the exact molecular weight of hyperbranched polyglycerol systems, interestingly, the difference in their molecular weights corresponds to that of the degradation products (i.e., 30 mercaptoethanol molecules). Therefore, we concluded that P(G-*b*-SSG) releases mercaptoethanol from the outer shell on degradation (Fig. S9 in the Supporting Information).

In order to observe the complex degradation of the core-degradable hyperbranched block copolymer P(SSG-*b*-G), we first studied the degradation mechanism of the PSSG homopolymer. In our previous work, we gained mechanistic insights on the degradation of PSSG polymers.<sup>21</sup> These were based on the presence of two possible reaction sites in SSG: the secondary alcohol and the disulfide linked primary alcohol.<sup>18</sup> Here, we have further studied the detailed structure of

the PSSG homopolymers by NMR spectroscopy to study polymer degradation (see Fig. S10 and Table S1 in the Supporting Information). During polymerization of the SSG monomer, there are two possible reaction routes for the hydroxyl groups that affect the direction of propagation of the growing polymer chain. For example, if a secondary alkoxide group is propagated, the polymer chain attaches to an epoxide unit and a linear 1,3-unit (L<sub>1,3</sub>) is generated; in contrast, a linear 1,11-unit (L<sub>1,11</sub>) is formed if a primary alkoxide reacts (Fig. 5). Although it is reported that the primary alkoxides (L<sub>1,4</sub>) are almost threefold more reactive than secondary alkoxides (L<sub>1,3</sub>) for anionic ring-opening multibranching polymerizations of a pure PG system,<sup>9</sup> PSSG shows the opposite tendency, to our surprise. Specifically, in the case of PSSG<sub>30</sub>, we found that the secondary alcohol (L<sub>1,3</sub>) is 1.71 times more reactive than the primary alcohol (L<sub>1,11</sub>) (Supporting Information Table S1). We propose that this observed difference in reactivity is mainly due to the relatively slow proton exchange that occurs in the long spacer unit of RCH<sub>2</sub>CH<sub>2</sub>S-SCH<sub>2</sub>CH<sub>2</sub>OH; thus, to exchange the proton, attack by an oxyanion is preferred entailing at the neighboring epoxide monomer. Supporting Information Figure S10 shows the expected chemical structure of PSSG<sub>30</sub>, considering the reactivity differences between the primary and secondary alcohols. As shown in Supporting Information Figure S11, after degradation, a large core segment is left with a molecular weight of 2281 g/mol, which closely corresponds to the value derived from GPC (2780 g/mol), as shown in Figure 4(b).

### Biocompatibility Test

We evaluated the cytotoxicity of PSSG<sub>30</sub>, P(SSG<sub>30</sub>-*b*-G<sub>50</sub>), P(SSG<sub>30</sub>-*b*-G<sub>100</sub>), and P(G<sub>130</sub>-*b*-SSG<sub>80</sub>) to investigate their potential for biomedical uses. Although our previous studies have indicated that the SSG monomer does not have an adverse effect on cells when copolymerized with G, here, we have focused more on differences in cell viability with

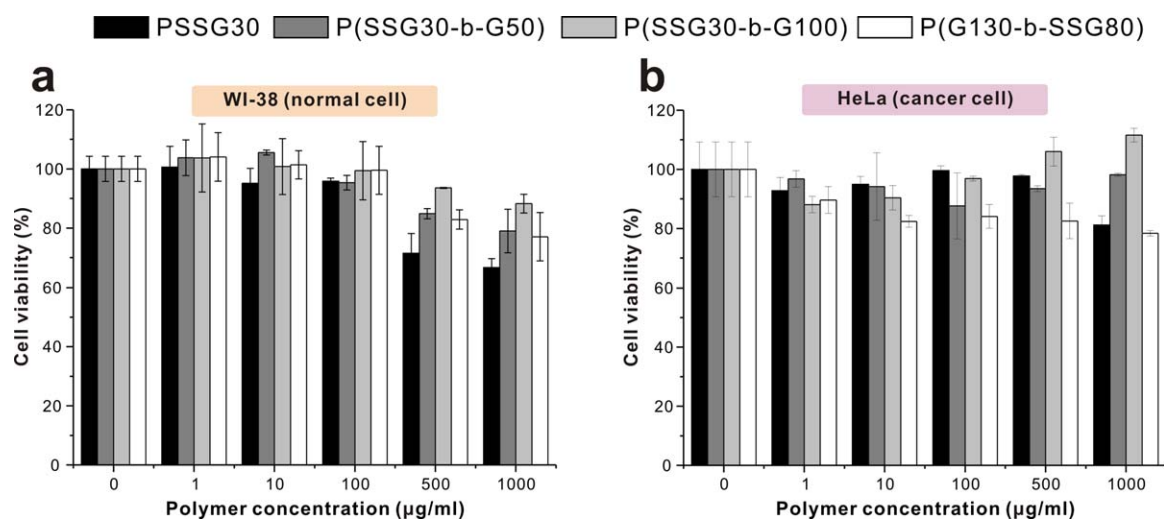


**FIGURE 6** *In vitro* cell viability assays of PSSG<sub>30</sub> (black), P(SSG<sub>30</sub>-*b*-G<sub>50</sub>) (dark grey), P(SSG<sub>30</sub>-*b*-G<sub>100</sub>) (grey), and P(G<sub>130</sub>-*b*-SSG<sub>80</sub>) (white) polymers determined by MTT assay using (a) WI-38 (normal cell) and (b) HeLa (cancer cell). [Color figure can be viewed in the online issue, which is available at [wileyonlinelibrary.com](http://wileyonlinelibrary.com).]

respect to the position of the disulfide bonds in the polymers. As shown in Figure 6, cells exposed to PSSG<sub>30</sub>, P(SSG<sub>30</sub>-*b*-G<sub>50</sub>), and P(SSG<sub>30</sub>-*b*-G<sub>100</sub>), which have an identical PSSG core, showed increasing cell viability with increasing G content. This can be explained by the non-toxic PG chains that encircle the PSSG core as G content increases. In contrast, P(G<sub>130</sub>-*b*-SSG<sub>80</sub>) causes cells to have lower viability than P(SSG<sub>30</sub>-*b*-G<sub>100</sub>) because SSG is exposed at the outer shell. In addition, although the unstable disulfide bond in P(SSG-*b*-G) can be converted to thiol or thioether under polymerization conditions, disulfide bonds in P(G-*b*-SSG) remain, leading to the higher biocompatibility of P(SSG-*b*-G) than P(G-*b*-SSG).

## CONCLUSIONS

Homopolymers and block copolymers of hyperbranched redox-degradable PGs were successfully synthesized by anionic ring-opening, multibranching polymerization using the redox degradable SSG monomer containing disulfide bonds and the non-degradable G monomer. All of the synthesized polymers were characterized by <sup>1</sup>H NMR spectroscopy, GPC, and DSC measurements, and these indicated well-controlled molecular weight and narrow polydispersity. Side reactions of the disulfide bond during polymerization, which are important in redox-responsive systems, were characterized by free thiol titration experiments, which demonstrated that thiol groups generated by side reactions of the disulfide bond during polymerization exist in the final polymer. Moreover, we found that P(SSG-*b*-G) contains more thiol groups than either PSSG or P(G-*b*-SSG). We also explored the structures of the degradation products of a series of redox-degradable hyperbranched PGs using <sup>1</sup>H NMR, and GPC measurements. We found that the structure of the degradation products of P(G-*b*-SSG) and P(SSG-*b*-G) are different, and we have suggested a degradation mechanism based on the structure of the PSSG homopolymer. *In vitro* cytotoxicity

studies revealed the decent biocompatibility of homopolymers and block copolymers of hyperbranched redox-degradable PGs. We anticipate that our research will extend the structural diversity of PG based polymers and help the understanding of the structure of degradable PG systems.

## ACKNOWLEDGMENTS

This work was supported by the National Research Foundation of Korea (NRF) grant (No. 2010-0028684) and by the 2014 Research Fund (1.140101.01) of Ulsan National Institute of Science and Technology (UNIST).

## REFERENCES AND NOTES

- 1 D. Wilms, S. E. Stiriba, H. Frey, *Acc. Chem. Res.* **2009**, *43*, 129–141.
- 2 H. Frey, R. Haag, *R. Rev. Mol. Biotechnol.* **2002**, *90*, 257–267.
- 3 A. Thomas, S. S. Müller, H. Frey, *Biomacromolecules* **2014**, *15*, 1935–1954.
- 4 R. K. Kainthan, J. Janzen, E. Levin, D. V. Devine, D. E. Brooks, *Biomacromolecules* **2006**, *7*, 703–709.
- 5 M. C. Lukowiak, S. Wettmarshausen, G. Hidde, P. Landsberger, V. Boenke, K. Rodenacker, U. Braun, J. F. Friedrich, A. A. Gorbushina, R. Haag, *Polym. Chem.* **2015**, *6*, 1350–1359.
- 6 R. K. Kainthan, J. Janzen, J. N. Kizhakkedathu, D. V. Devine, D. E. Brooks, *Biomaterials* **2008**, *29*, 1693–1704.
- 7 S. Lee, K. Saito, H. R. Lee, M. J. Lee, Y. Shibasaki, Y. Oishi, B. S. Kim, *Biomacromolecules* **2012**, *13*, 1190–1196.
- 8 S. Son, E. Shin, B. S. Kim, *Biomacromolecules* **2014**, *15*, 628–634.
- 9 A. Sunder, R. Hanselmann, H. Frey, R. Mülhaupt, *Macromolecules* **1999**, *32*, 4240–4246.
- 10 R. A. Shenoi, D. E. Brooks, J. N. Kizhakkedathu, *J. Polym. Sci. Part A: Polym. Chem.* **2013**, *51*, 2614–2621.

- 11** C. Mangold, F. Wurm, H. Frey, *Polym. Chem.* **2012**, *3*, 1714–1721.
- 12** M. Erberich, H. Keul, M. Möller, *Macromolecules* **2007**, *40*, 3070–3079.
- 13** Y. Oikawa, S. Lee, D. H. Kim, D. H. Kang, B. S. Kim, K. Saito, S. Sasaki, Y. Oishi, Y. Shibasaki, *Biomacromolecules* **2013**, *14*, 2171–2178.
- 14** F. Paulus, D. Steinhilber, P. Welker, D. Mangoldt, K. Licha, H. Depner, S. Sigrüst, R. Haag, *Polym. Chem.* **2014**, *5*, 5020–5028.
- 15** C. Schüll, T. Gieshoff, H. Frey, *Polym. Chem.* **2013**, *4*, 4730–4736.
- 16** B. F. Lee, M. J. Kade, J. A. Chute, N. Gupta, L. M. Campos, G. H. Fredrickson, E. J. Kramer, N. A. Lynd, C. J. Hawker, *J. Polym. Sci. Part A: Polym. Chem.* **2011**, *49*, 4498–4504.
- 17** A. Lee, P. Lundberg, D. Klinger, B. F. Lee, C. J. Hawker, N. A. Lynd, *Polym. Chem.* **2013**, *4*, 5735–5742.
- 18** K. M. Mattson, A. A. Latimer, A. J. McGrath, N. A. Lynd, P. Lundberg, Z. M. Hudson, C. J. Hawker, *J. Polym. Sci. Part A: Polym. Chem.* **2015**, *53*, 2685–2692.
- 19** R. A. Shenoi, J. K. Narayanannair, J. L. Hamilton, B. F. Lai, S. Horte, R. K. Kainthan, J. P. Varghese, K. G. Rajeev, M. Manoharan, J. N. Kizhakkedathu, *J. Am. Chem. Soc.* **2012**, *134*, 14945–14957.
- 20** R. A. Shenoi, B. F. Lai, M. Imran ul-haq, D. E. Brooks, J. N. Kizhakkedathu, *Biomaterials* **2013**, *34*, 6068–6081.
- 21** S. Son, E. Shin, B. S. Kim, *Macromolecules* **2015**, *48*, 600–609.
- 22** J. T. Wiltshire, G. G. Qiao, *Macromolecules* **2008**, *41*, 623–631.
- 23** C. C. Chang, T. Emrick, *Macromolecules* **2014**, *47*, 1344–1350.
- 24** J. T. Wiltshire, G. G. Qiao, *Macromolecules* **2006**, *39*, 9018–9027.
- 25** R. Nicolaÿ, L. Marx, P. Hémerly, K. Matyjaszewski, *Macromolecules* **2007**, *40*, 9217–9223.
- 26** A. C. Engler, J. M. Chan, K. Fukushima, D. J. Coady, Y. Y. Yang, J. L. Hedrick, *ACS Macro Lett.* **2013**, *2*, 332–336.
- 27** M. Rikkou-Kalourkoti, K. Matyjaszewski, C. S. Patrickios, *Macromolecules* **2012**, *45*, 1313–1320.
- 28** A. J. Parker, N. Kharasch, *Chem. Rev.* **1959**, *59*, 583–627.
- 29** R. G. Hiskey, A. J. Dennis, *J. Org. Chem.* **1968**, *33*, 2734–2738.
- 30** J. P. Danehy, M. Y. Oester, *J. Org. Chem.* **1967**, *32*, 1491–1495.
- 31** M. Desroches, S. Caillol, V. Lapinte, R. Auvergne, B. Boutevin, *Macromolecules* **2011**, *44*, 2489–2500.